

## **SUPPLEMENTARY INFORMATION CONTENT**

### **I. Supplementary Materials and Methods**

### **II. Supplementary Figures**

**Figure S1.** Association of HF-RPL18 with polysome complexes.

**Figure S2.** Results of *in situ* hybridizations confirms transgene expression in distinct cell domains during flower development.

**Figure S3.** Sensitivity, linearity and reproducibility.

**Figure S4.** Domain-specific genes for flower stages 6-7.

**Figure S5.** Comparison of domain-specific genes during early flower development with other datasets.

**Figure S6.** Cell-specific involvement of gene functions.

**Figure S7.** Cellular distributions of C2C2-GATA transcription factor genes.

**Figure S8.** Cell-specific enrichment of transcription factor families.

**Figure S9.** Limited correlation between intron levels and transcript levels.

**Figure S10.** Slightly reduced UA richness in retained introns.

**Figure S11.** Correlation of gene transcript features and IR.

**Figure S12.** Relationship between gene function and IR.

**Figure S13.** Fine-tuning of development-related genes.

**Figure S14.** 5' mRNA folding energy correlates with translation state.

**Figure S15.** Relationship between gene function and translation state.

**Figure S16.** Semi-quantitative RT-PCR analysis of ribosome-associated ncRNA.

### **III. Supplementary Tables**

**Table S1.** Summary of mapped reads and replicates for each experiment.

**Table S2.** Length, sequences, and dilution of spike-in RNA molecules.

**Table S3.** Flower-specific genes with *in situ* hybridization data in the literature used in Figure 1C.

**Table S4.** Domain-specific genes at flower stage 4.

**Table S5.** Domain-specific genes at flower stages 6-7.

**Table S6.** Stage-specific genes between stages 4 and 6-7.

**Table S7.** Hormone responsive genes used for meta analysis.

**Table S8.** Expression of splicing isoforms in each spatiotemporal point.

**Table S9.** Novel splicing isoforms detected during early flower development.

**Table S10.** Detected introns and their levels.

**Table S11.** 5' mRNA folding energy correlates with translation efficiency at different window size.

**Table S12.** Polysome-associated ncRNAs, their spatiotemporal expression, and RFC scores.

**Table S13.** Transcription factor genes used for meta analysis.

**Table S14.** Primers used for RT-PCR of ribosome-associated ncRNA.

## SUPPLEMENTARY MATERIALS AND METHODS

### Plasmids and DNA cloning

DNA cloning was performed following standard procedures (Sambrook et al., 1989) using *Escherichia coli* strain DH5 $\alpha$ .

The HF-RPL18 coding sequence was isolated as a *KpnI/XbaI* fragment from pGATA 35S::HF-RPL18 (Zanetti *et al*, 2005) and inserted into the BJ36 vector. The resulting construct was named BJ36 HF-RPL18. The *Arabidopsis* AP1 promoter was PCR amplified from genomic DNA as a 5,000-bp fragment with added *XhoI* and *KpnI* sites and inserted into BJ36 HF-RPL18. The entire pAP1::HF-RPL18::tOCS cassette was then released by *NotI* and subcloned into the pMLBart binary vector. Similarly, the AP3 promoter was PCR amplified from pD1954 (Jack et al., 1994) as a 3,800-bp fragment with added *SalI/XhoI* sites and inserted into BJ36 HF-RPL18. The RPL18 promoter was PCR amplified from genomic DNA as a 4,000-bp fragment 5' to the ORF start codon of *AtRPL18B* (At3g05590) with added *XhoI* and *KpnI* sites and inserted into BJ36 HF-RPL18. Both pAP3::HF-RPL18::tOCS cassette and pRPL18::HF-RPL18::tOCS cassette were released by *NotI* and subcloned into the pMLBart binary vector.

The EF HF-RPL18 construct was generated by introducing the HF-RPL18 coding sequence as a blunt-ended *KpnI/XbaI* fragment from pGATA 35S::HF-RPL18 (Zanetti *et al*, 2005) into the blunt-ended *SalI* site of the binary vector pV-TOP under the control of pOp (6x) promoter (Craft *et al*, 2005). A pre-existing GUS reporter gene is driven by the same pOp (6x) operator array for divergent expression in pV-TOP.

## Plant lines, growth, crosses, and selection

The *Arabidopsis thaliana* ecotype Landsberg *erecta* was used in this study.

35S::AP1-GR *ap1-1 cal-1* plants (Wellmer et al., 2006) were germinated on MS medium supplemented with 50 mg L<sup>-1</sup> kanamycin (Sigma-Aldrich, St. Louis, MO), and pAG::LhG4 plants (Lenhard *et al.*, 2001) were germinated on MS medium supplemented with 25 mg L<sup>-1</sup> phosphinothricin (Sigma-Aldrich, St. Louis, MO).

All binary vector constructs were introduced into *Agrobacterium tumefaciens* strain GV3101 by electroporation, and 35S::AP1-GR *ap1-1 cal-1* plants were transformed by floral dip (Clough and Bent, 1998) except EF HF-RPL18, which was transformed into pAG::LhG4 plants. Primary transformants were selected on medium containing 25 mg L<sup>-1</sup> phosphinothricin or 35 mg L<sup>-1</sup> hygromycin, respectively, and inspected for growth aberrations during their further development. In the T<sub>2</sub> generation, lines were selected that showed a 3:1 segregation ratio for the transgene. To select pAP1::HF-RPL18, pAP3::HF-RPL18, and pRPL18::HF-RPL18 lines, flowers of 20 preselected T<sub>2</sub> plants were collected and HF-RPL18 protein levels were quantified by Western blotting. Blots were probed with anti-FLAG M2 monoclonal antibodies (Sigma-Aldrich, St. Louis, MO). Three lines with the highest intensity were selected for each construct. Finally, in situ hybridizations were performed to confirm the expected expression domains of HF-RPL18. Non-radioactive in situ hybridizations were performed as previously described (Wellmer et al., 2006). A detailed in situ hybridization protocol can be found at <http://www.its.caltech.edu/~plantlab/html/protocols.html>). For RNA probe synthesis, a 155-bp sequence (TCATACCGGATCCACCTCCTCCACCACCTCCCTTATCATCATCATCCTTATAA

TCACCTCCACCATGGTGATGATGGTGATGTCCCATGGTAATTGTAAATGTAAT  
TGTAATGTTGTTTGTGTTGTTTGTGTTGTTGGTAATTGTTGTAAAATAG) against  
the His-FLAG region of HF-RPL18 was PCR amplified and ligated into the pCR2.1-  
TOPO vector (Invitro, Carlsbad, CA), and the resulting constructs were sequenced to  
determine the orientation of the inserts. All lines showed the expected expression  
patterns. One line for each construct (pAP1::HF-RPL18 #3, pAP3::HF-RPL18 #19, and  
pRPL18::HF-RPL18 #8) with the strongest in situ hybridization signal was chosen for  
subsequent analysis. The selected line with pAP1::HF-RPL18 was tested for HF-RPL18  
distribution in polysomes of different sizes as assessed by sucrose density gradient  
centrifugation (see below). Western blotting with anti-FLAG M2 monoclonal antibodies  
confirmed the expected equal incorporation of HF-RPL18 in polysomes of different sizes  
(Figure S1), which is consistent with Zanetti et al, 2005. These lines are submitted to the  
ABRC stock center.

To select EF HF-RPL18 plants, flowers of 96 preselected T<sub>2</sub> plants were screened  
for GUS activity. Twelve lines with the AG-like staining pattern, as well as the highest  
staining intensity and frequency were chosen for HF-RPL18 protein quantification by  
Western blotting as described above. Finally, one line (pAG::LhG4; pOp::HF-RPL18, or  
pAG>>HF-RPL18 #51) with the strongest protein levels were confirmed by in situ  
hybridization of HF-RPL18 expression as described above. Genetic crosses of the  
pAG>>HF-RPL18 line were performed with homozygous 35S::AP1-GR *ap1-1 cal-1*  
plants. F<sub>1</sub> progeny were selected that contained all three T-DNAs. A plant homozygous  
for all three T-DNAs and both mutants were selected from the F<sub>3</sub> generation based on the

*ap1-1 cal-1* phenotype and the segregation ratio of the transgenes. This line has been submitted to the ABRC stock center.

### **Microarray experiment**

The microarray platform, probe labeling, array hybridization, and data processing were performed as previously described (Wellmer et al., 2006). Briefly, the same RNA samples purified from the AP1 domain and from entire floral tissue (using pRPL18::HF-RPL18 plants) at stage 4, which were used for RNA-seq, were amplified, labeled, and hybridized to 70-mer oligonucleotide microarray slides two times with a dye swap. Spike-in control RNAs were added at the same concentration (Table S2) to both samples. Raw data were processed using the Resolver gene expression data analysis system version 4.0 (Rosetta Biosoftware, Seattle, Washington, United States) as described previously (Wellmer et al., 2006) to obtain normalized expression levels.

### **Spike-in RNA control**

Ten spike-in RNA control molecules were either obtained from Ambion (Austin, TX) or in vitro transcribed (SPIKE\_AM1S, SPIKE\_L2,3-2 and SPIKE\_L1-1) using the MAXIscript T7 Kit (Ambion) following the same protocol for in situ hybridization probe synthesis. The integrity of the RNA was inspected on a 1.5% agarose gel stained with ethidium bromide under UV light. These spike-in RNA control range from 498-nt to 11,936-nt, representing the size distribution of *Arabidopsis* mRNAs. Serial dilutions were made to the concentrations indicated. The number of each spike-in added to a

library and the exact sequence are available in Table S2. Complementary 70-mer oligos were also printed on microarray slides for all spike-in RNA controls except SPIKE\_L2,3-2 and SPIKE\_L1-1.

### **Gene enrichment analysis**

The lists of the phytohormone-responsive genes were based on the AtGenExpress hormone treatment data set (Goda et al, 2008) and the Arabidopsis Hormone Database (Peng et al, 2009). Hormone-responsive gene lists from both sources were combined and provided in Table S7. Transcription factor annotation and classification were based on three databases, AGRIS, DATF and RARTF (Guo et al, 2005; Iida et al, 2005; Palaniswamy et al, 2006). A gene is considered a transcription factor family member if it was annotated by at least two of the three databases. The lists of transcription factor genes are available in Table S13. The enrichment analysis was performed as previously described in Sugimoto et al, 2010. To determine which categories of hormone-responsive genes or transcription factor genes (HT) are enriched with cell domain or flower stage specific (CF) genes, the number of CF genes contained in each HT category was counted. Log odds-ratio ( $LR$ ) was calculated to quantify enrichment:

$$LR = \log_2\left(\frac{q/k}{m/t}\right),$$

where  $q$  is the count of CF genes in an HT category,  $k$  is the total number of CF genes,  $m$  is the total number of an HF category, and  $t$  is the total number of annotated genes.

Permutation tests were used to assess the statistical significance ( $P$  value) of CF gene enrichment in each HT category. In each Monte Carlo simulation, we randomly selected

the same number of CF genes and the same number of genes as each category from all expressed genes and then calculated the overlapping portion. Across 1E+6 such simulations, the overlapping portions were all distributed in accordance with the Student's t test distribution. A one-sided  $P$  value was calculated as the fraction of 1E+6 Monte Carlo simulation values that are at least as extreme as the original statistic observed from experiments.  $P$  values less than 1E-06 were computed from the hypergeometric distribution. To control the false discovery rate (FDR) for the above enrichment tests,  $Q$  values were calculated. FDR was assessed at below 5E-04 at the  $P$  value cutoff of 1E-04.

### **Promoter motif analysis**

Motif search was performed as described before (Jiao et al, 2005). The genome sequences 2 kb upstream of annotated translation start sites were retrieved from the TAIR9 genome build. Both DNA strands were searched using Sift, an enumerative algorithm (Hudson and Quail, 2003; <http://stan.cropsci.uiuc.edu/tools.php>). Only elements meeting the critical  $E$  value smaller than  $10^{-4}$  were selected. Comparison of detected motifs with known motifs was performed using Elefinder of the Sift package.

### **Comparison with leaf data**

Translation state data for *Arabidopsis* rosette leaves were obtained from Kawaguchi and Bailey-Serres, 2005. Genes with the highest and lowest (10%) ribosome loading (RL) values under non-stress (NS) or dehydration stress (DS) were compared with our highly translated and weakly translated genes in flowers ( $\geq 2$  fold and  $P < 0.001$ ). Overlapping



and significance tests were performed as described above. We found only 54 (NS) and 71 (DS) genes were highly translated in both leaves and flowers, and 33 (NS) and 15 (DS) genes were weakly translated in both tissues. These numbers were not significantly different from randomized data ( $P \approx 0.9$ ).

### **Polysome separation**

Inflorescence tissue (~0.2 g) was ground to fine powder in liquid nitrogen, and homogenized in 1.25 ml ice-cold polysome extraction buffer (previously described for immunopurification of polysomes). The brei was clarified by centrifuging for 10 min at  $16,000 \times g$ ,  $4^{\circ}\text{C}$ . The polysomes were pelleted from the supernatant through a 3.5 ml layer of 1.6 M sucrose (in 40 mM trizma, pH 8.4; 20 mM KCl; and 21 mM  $\text{MgCl}_2$ ) at  $170,000 \times g$ ,  $4^{\circ}\text{C}$ , for 18 hr in a Beckman 70Ti rotor. The pellets were recovered by aspirating the supernatant from the centrifuge tubes. The pellets were resuspended in the polysome extraction buffer for 1 hr at  $4^{\circ}\text{C}$  on a shaker. The suspensions were then layered on gradients equilibrated in polyallomer centrifuge tubes. The gradients were formed by layering 0.75, 1.50, 1.50 and 0.75 ml of 60%, 45%, 30% and 20% sucrose (in 40 mM trizma, pH 8.4; 20 mM KCl; and 21 mM  $\text{MgCl}_2$ ). Gradients were allowed to equilibrate for at least 16 hr at  $4^{\circ}\text{C}$  before use. The preparations were centrifuged in a Beckman SW55Ti rotor at  $275,000 \times g$ ,  $4^{\circ}\text{C}$  for 1.5 hr. The gradients were analyzed with an ISCO gradient fractionator linked to an A260 nm UV absorbance monitor. Fractions for non-polysome (NP) and polysome (PS, two or more ribosomes per mRNA) were combined respectively for further analysis as suggested in Kawaguchi et al, 2003 and 2004 (Figure S16A).

For RNA isolation, RNA was precipitated by adding an equal volume of 8M guanidine HCl and 1.5 volume of ethanol at -20°C for at least 16 hr. After centrifugation at 16,000 × g, 4°C for 45 min, the RNA pellet was resuspended in water and purified using RNeasy kit (Qiagen, Valencia, CA) following the manufacture's protocol.

## **RT-PCR**

1 µg of total RNA isolated from separated polysome NP or PS fractions was reverse-transcribed with SuperScript III (Invitrogen, Carlsbad, CA). 0.5-1% of the resulting cDNA was subjected to PCR. The primer sets are listed in Table S14, and 30 cycles were used for amplification.

## **SUPPLEMENTARY REFERENCES**

Clough SJ, Bent AF (1998) Floral dip: a simplified method for *Agrobacterium*-mediated transformation of *Arabidopsis thaliana*. *Plant J* **16**: 735-743.

Craft J, Samalova M, Baroux C, Townley H, Martinez A, Jepson I, Tsiantis M, Moore I (2005) New pOp/LhG4 vectors for stringent glucocorticoid-dependent transgene expression in *Arabidopsis*. *Plant J* **41**: 899-918.

Goda H, Sasaki E, Akiyama K, Maruyama-Nakashita A, Nakabayashi K, Li W, Ogawa M, Yamauchi Y, Preston J, Aoki K, Kiba T, Takatsuto S, Fujioka S, Asami T, Nakano T, Kato H, Mizuno T, Sakakibara H, Yamaguchi S, Nambara E, et al. (2008) The AtGenExpress hormone and chemical treatment data set: experimental design, data evaluation, model data analysis and data access. *Plant J* **55**: 526-542.

Guo A, He K, Liu D, Bai S, Gu X, Wei L, Luo J (2005) DATF: a database of *Arabidopsis* transcription factors. *Bioinformatics* **21**: 2568-2569.

Hudson ME, Quail PH (2003) Identification of promoter motifs involved in the network of phytochrome A-regulated gene expression by combined analysis of genomic sequence and microarray data. *Plant Physiol* **133**: 1605-1616.

- Iida K, Seki M, Sakurai T, Satou M, Akiyama K, Toyoda T, Konagaya A, Shinozaki K (2005) RARTF: database and tools for complete sets of *Arabidopsis* transcription factors. *DNA Res* **12**: 247-256.
- Jack T, Fox GL, Meyerowitz EM (1994) *Arabidopsis* homeotic gene *APETALA3* ectopic expression: transcriptional and post-transcriptional regulation determine floral organ identity. *Cell* **76**: 703-716.
- Jiao Y, Ma L, Strickland E, Deng XW (2005) Conservation and divergence of light-regulated genome expression patterns during seedling development in rice and *Arabidopsis*. *Plant Cell* **17**: 3239-3256.
- Kawaguchi R, Girke T, Bray EA, Bailey-Serres J (2004) Differential mRNA translation contributes to gene regulation under non-stress and dehydration stress conditions in *Arabidopsis thaliana*. *Plant J* **38**: 823-839.
- Kawaguchi R, Williams AJ, Bray EA, Bailey-Serres J (2003) Translational regulation in response to water deficit stress in *Nicotiana tabacum*. *Plant Cell Environ* **26**: 221-229.
- Lenhard M, Bohnert A, Jurgens G, Laux T (2001) Termination of stem cell maintenance in *Arabidopsis* floral meristems by interactions between WUSCHEL and AGAMOUS. *Cell* **105**: 805-814.
- Palaniswamy SK, James S, Sun H, Lamb RS, Davuluri RV, Grotewold E (2006) AGRIS and AtRegNet. a platform to link cis-regulatory elements and transcription factors into regulatory networks. *Plant Physiol* **140**: 818-829.
- Peng ZY, Zhou X, Li L, Yu X, Li H, Jiang Z, Cao G, Bai M, Wang X, Jiang C, Lu H, Hou X, Qu L, Wang Z, Zuo J, Fu X, Su Z, Li S, Guo H (2009) *Arabidopsis* Hormone Database: a comprehensive genetic and phenotypic information database for plant hormone research in *Arabidopsis*. *Nucleic Acids Res* **37**: D975-982.
- Sambrook J, Fritsch E & Maniatis T (1989) *Molecular Cloning: A Laboratory Manual*. Cold Spring Harbour Press, Cold Spring Harbour, New York, USA
- Wellmer F, Alves-Ferreira M, Dubois A, Riechmann JL, Meyerowitz EM (2006) Genome-wide analysis of gene expression during early *Arabidopsis* flower development. *PLoS Genet* **2**: e117.
- Zanetti ME, Chang IF, Gong F, Galbraith DW, Bailey-Serres J (2005) Immunopurification of polyribosomal complexes of *Arabidopsis* for global analysis of gene expression. *Plant Physiol* **138**: 624-635.

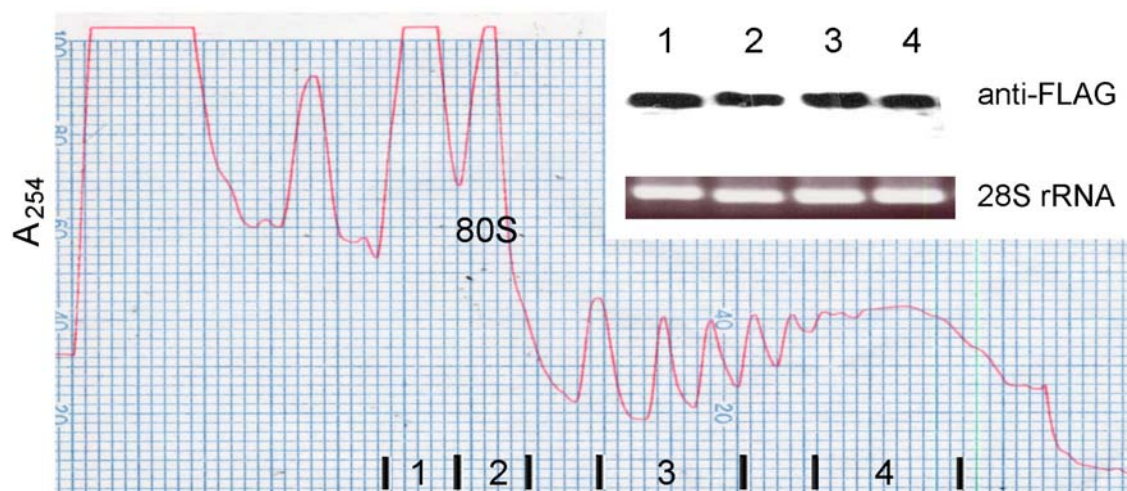


**Figure S1.** Association of HF-RPL18 with polysome complexes.

Flower stage 6-7 ribosomes from a pAP1::HF-RPL18 line were fractionated by ultracentrifugation through 20% to 60% (w/v) sucrose density gradients and the 254 nm UV absorbance profile was recorded. Ribosome concentration for fractions 1 through 4 was normalized based on RT-PCR of 28S rRNA and quantification results of 28S rRNA peaks using a Agilent 2100 bioanalyzer (not shown). The association of HF-RPL18 was analyzed by immunoblot analysis with  $\alpha$ -FLAG.

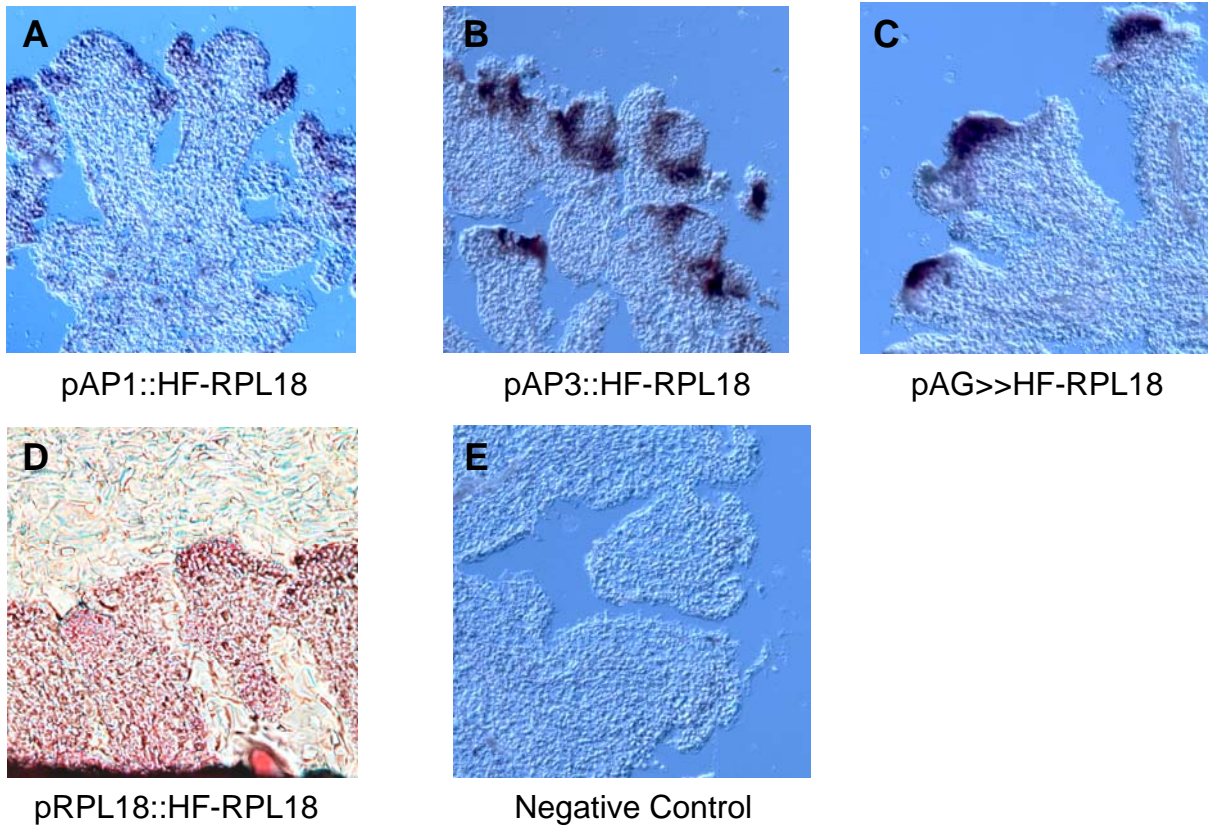


**Figure S2.** Results of *in situ* hybridizations confirms transgene expression in distinct cell domains during flower development.

Digoxigenin-labeled antisense RNA against His-FLAG tag sequences were hybridized to stage 5-6 flowers in lines expression *HF-RPL18* in AP1 (A), AP3 (B), AG (C) domains, and ubiquitously expressed under pRPL18 (D). A plant without *HF-RPL18* transgene was used as a negative control (E). All plant lines are in the 35S::AP1-GR *apl cal* background with dexamethasone induction.

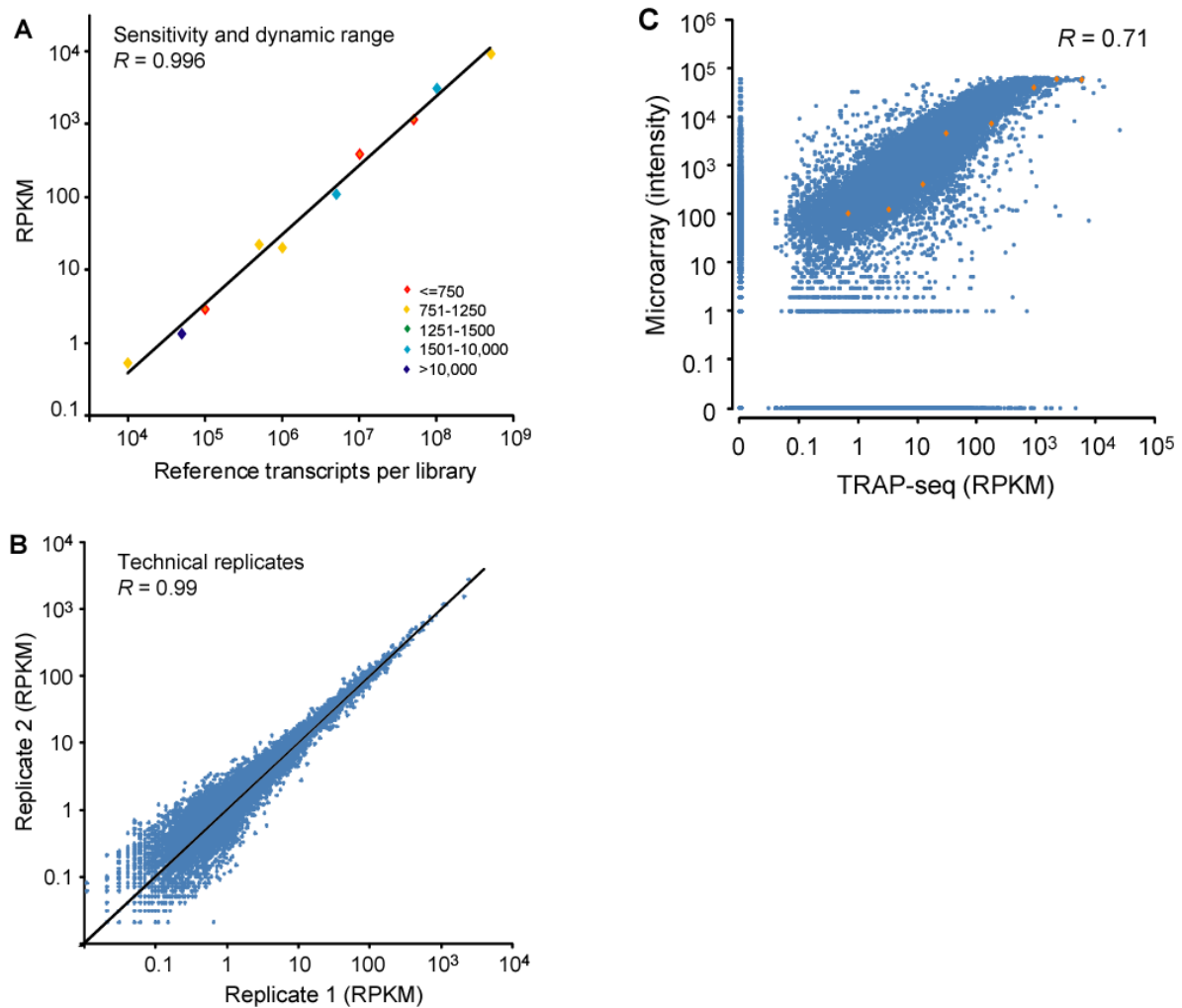


**Figure S3.** Sensitivity, linearity and reproducibility.

(A) Ten *in vitro* synthesized spike-in control transcripts of lengths 0.5-10 kb were added to the AP1, stage 4 RNA sample ( $1.0 \times 10^4$ - $1.0 \times 10^9$  transcripts per sample;  $R^2 = 0.99$ ). Spike-in controls are color-coded according to their length. (B) Comparison of two technical replicate AP1, stage 4 sample TRAP-Seq determinations for all TAIR9 gene models measured in RPKM ( $R^2 = 0.97$ ). (C) Signals from a 70-mer oligo microarray were compared with RNA-seq measurements. Same RNA samples were used for microarray and RNA-seq experiments. Spike-in controls spots are highlighted in orange.

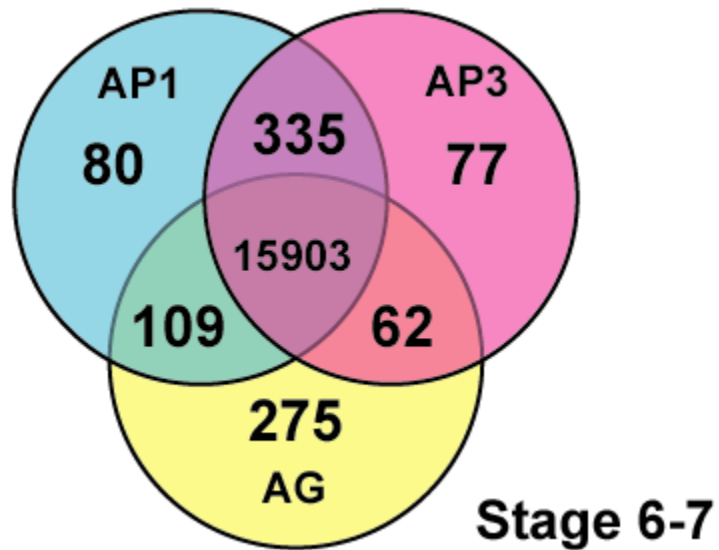


**Figure S4.** Domain-specific genes for flower stages 6-7.

Venn diagram of the cell domain-enriched genes that exhibited significant ( $\geq 2$ -fold with  $P < 0.001$ ) up-regulation as compared to the other domain(s) at stages 6-7. The numbers in middle areas indicate genes without domain-specific expression.

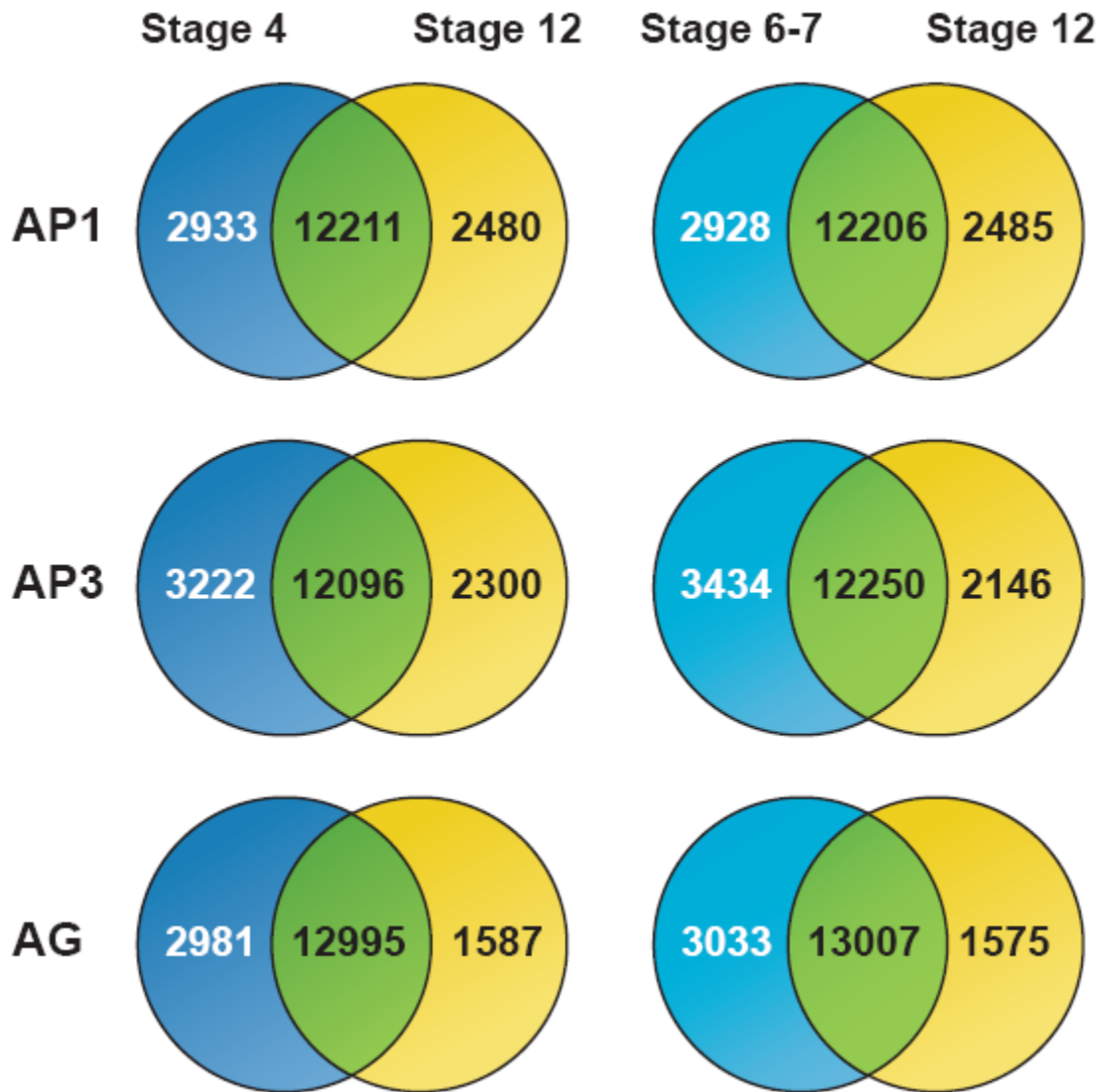
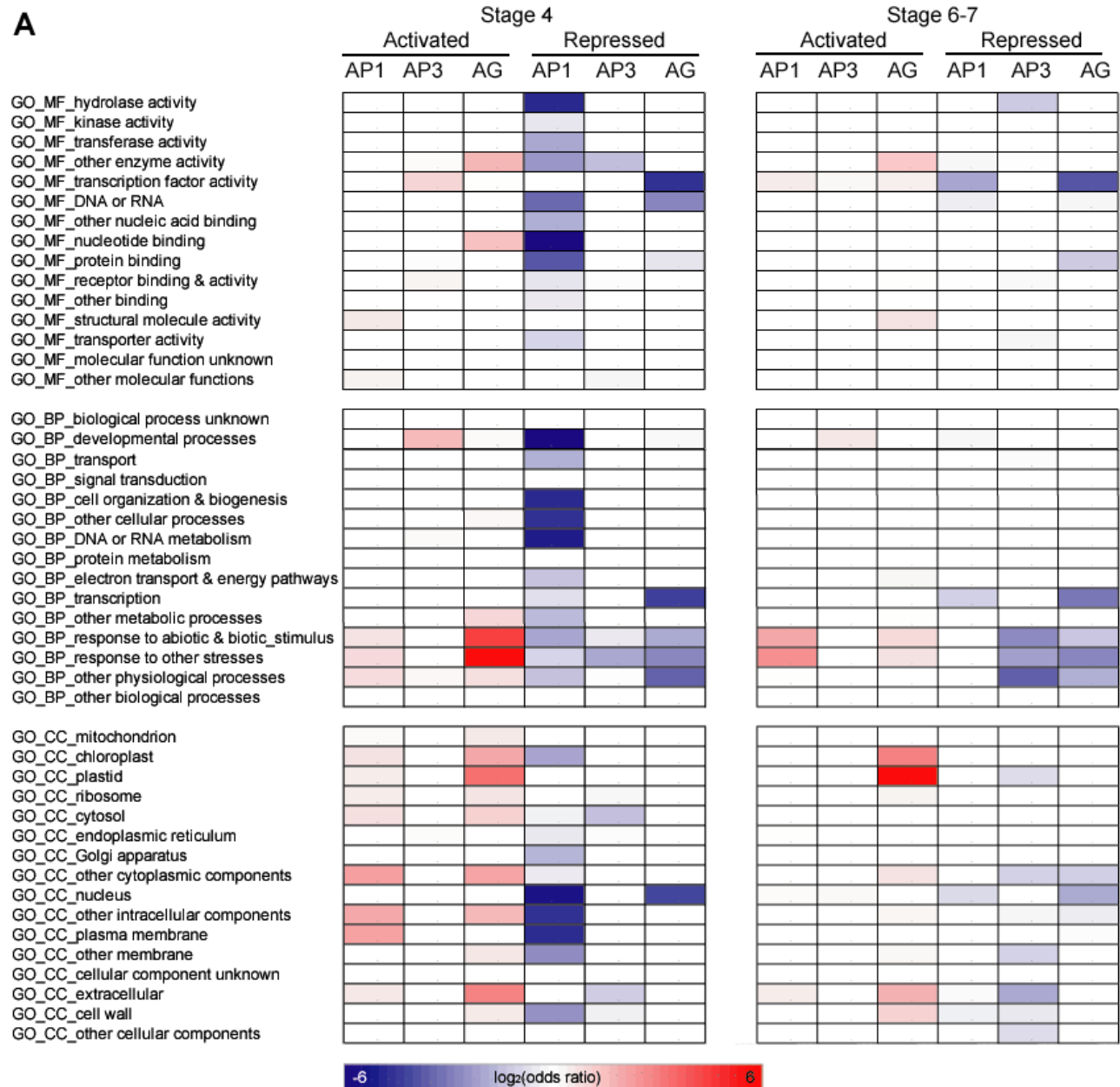


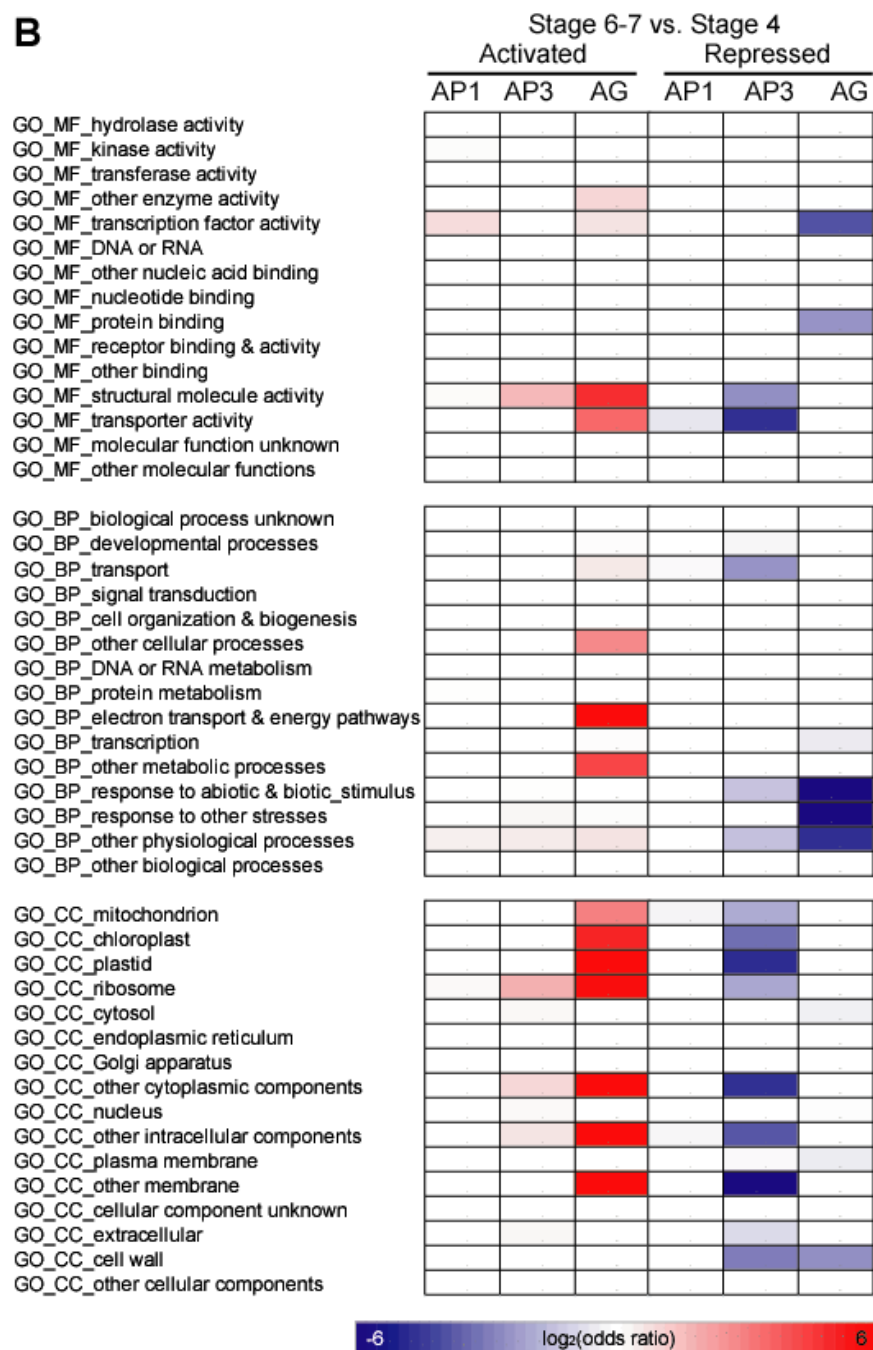
**Figure S5.** Comparison of domain-specific genes during early flower development with other datasets.

Venn diagrams illustrating both the overlapping and uniquely expressed gene numbers between each early stage (4 or 6-7) and stage 12 (Schmid et al., 2005). The numbers in overlapping areas show the shared gene number, while the numbers in non-overlapping areas show the unique gene number in both datasets.

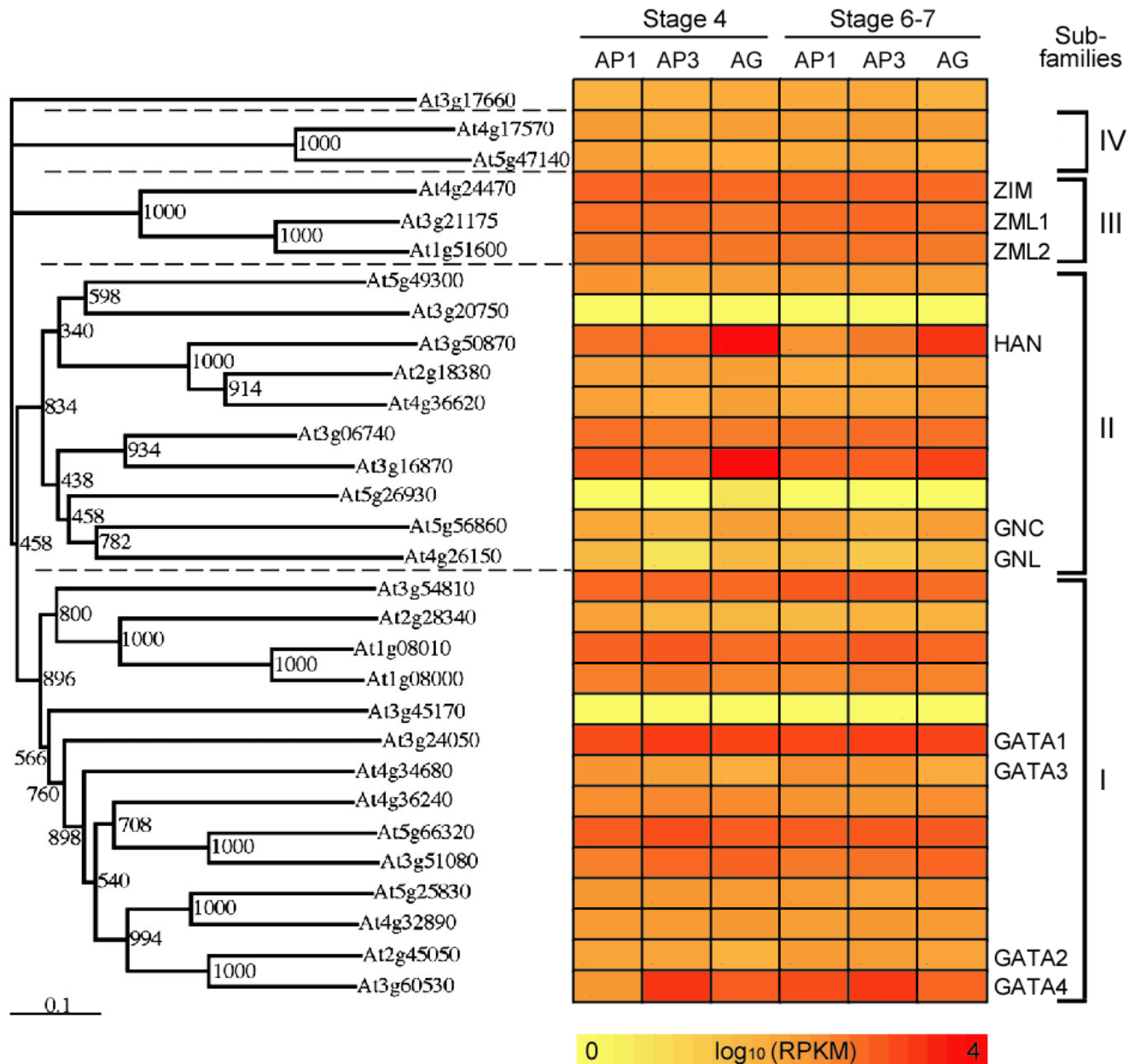


**A**



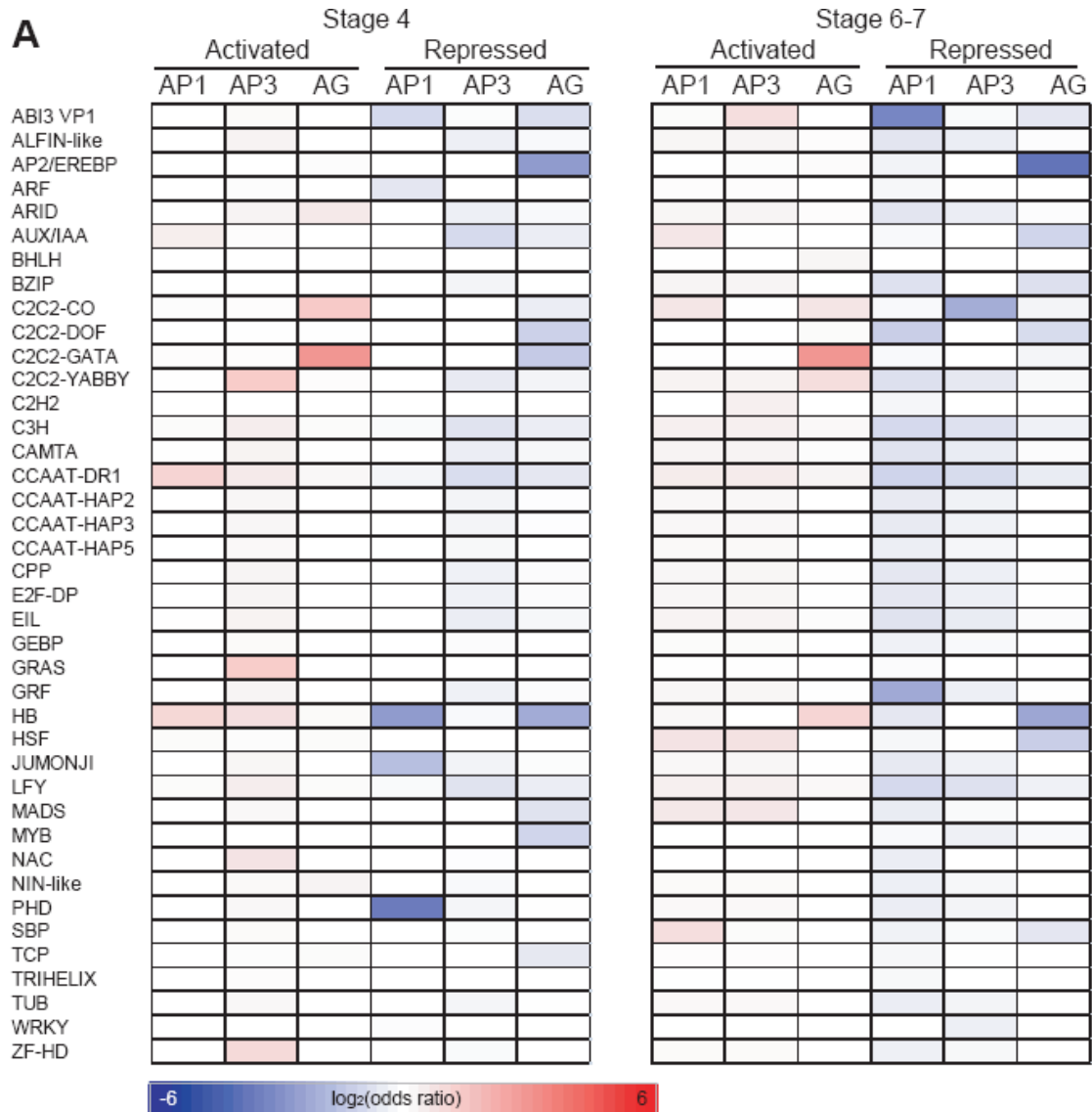
**B****Figure S6.** Cell-specific involvement of gene functions.

GO analysis identifies significantly overrepresented ( $P < 0.001$ ) gene categories in cell-specifically enriched or depleted genes at each stage (A), and in developmental stage-specific genes within each cell domain (B). Color bar: log<sub>2</sub>-transformed odds ratio of the enrichment of each GO category. Only categories with FDR corrected hypergeometric test  $P < 0.001$  are colored. MF: Molecular Function; BP: Biological Process; CC: Cellular Component.



**Figure S7.** Cellular distributions of C2C2-GATA transcription factor genes. Heat map representation of abundance of transcripts from C2C2-GATA transcription factor family genes in spatiotemporal samples. Classification and phylogeny of this family are based on Reyes et al., 2004.

**A**



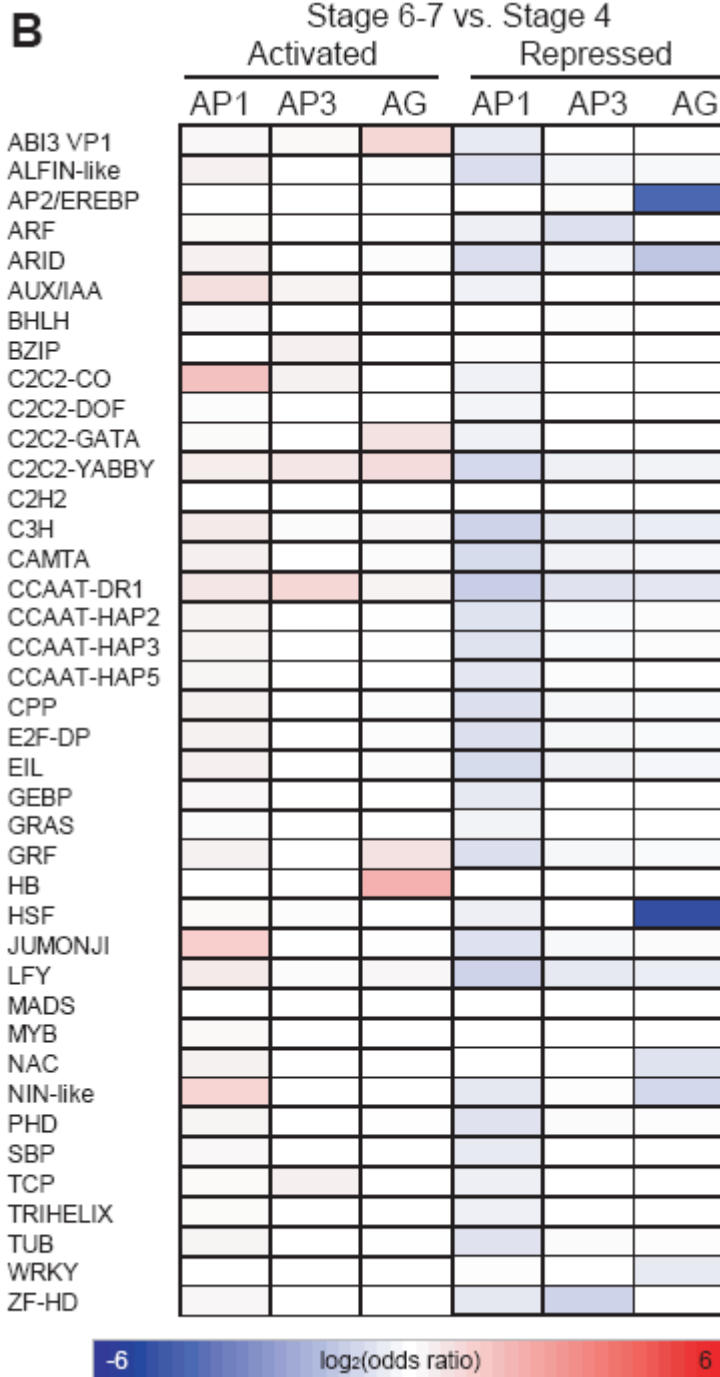


**Figure S8.** Cell-specific enrichment of transcription factor families.

Transcription factor families significantly overrepresented ( $P < 0.001$ ) gene categories in cell-specifically enriched or depleted genes at each stage (A), and in developmental stage-specific genes within each cell domain (B). Color bar: log<sub>2</sub>-transformed odds ratio of the enrichment of each family. Only families with FDR corrected hypergeometric test  $P < 0.001$  are colored.

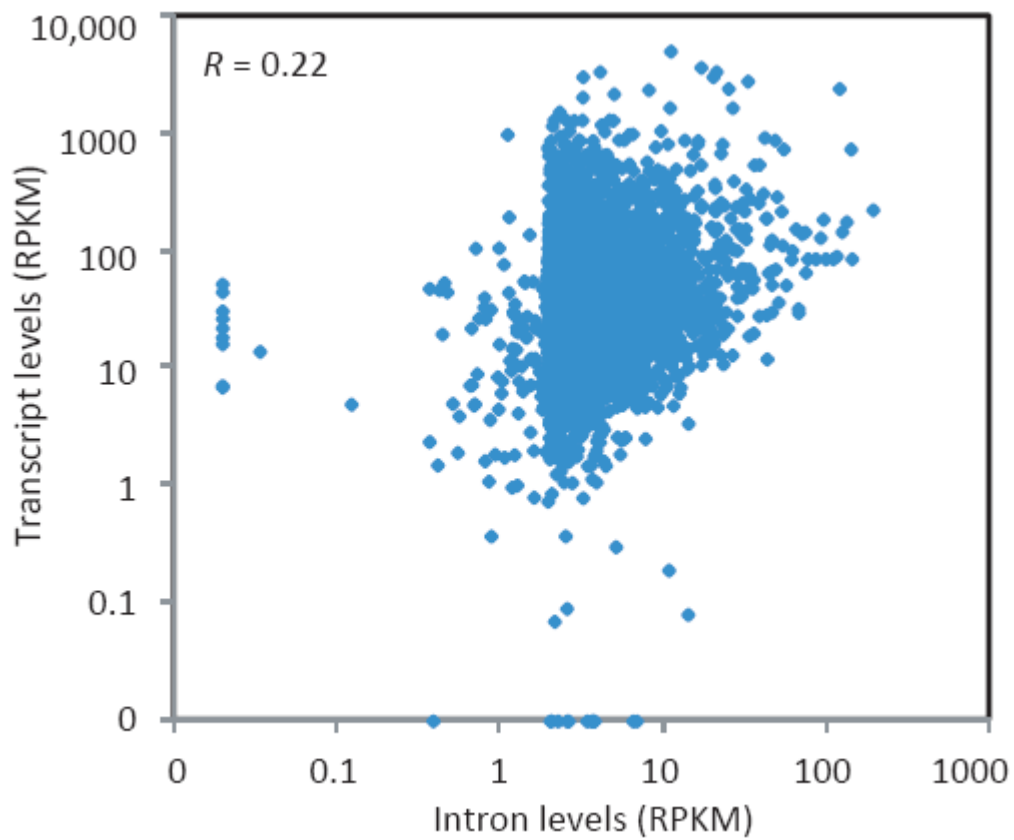


**Figure S9.** Limited correlation between intron levels and transcript levels.

Transcript levels are correlated with detected intron levels to a limited extent ( $R = 0.22$ ,  $P = 10^{-3}$ ).

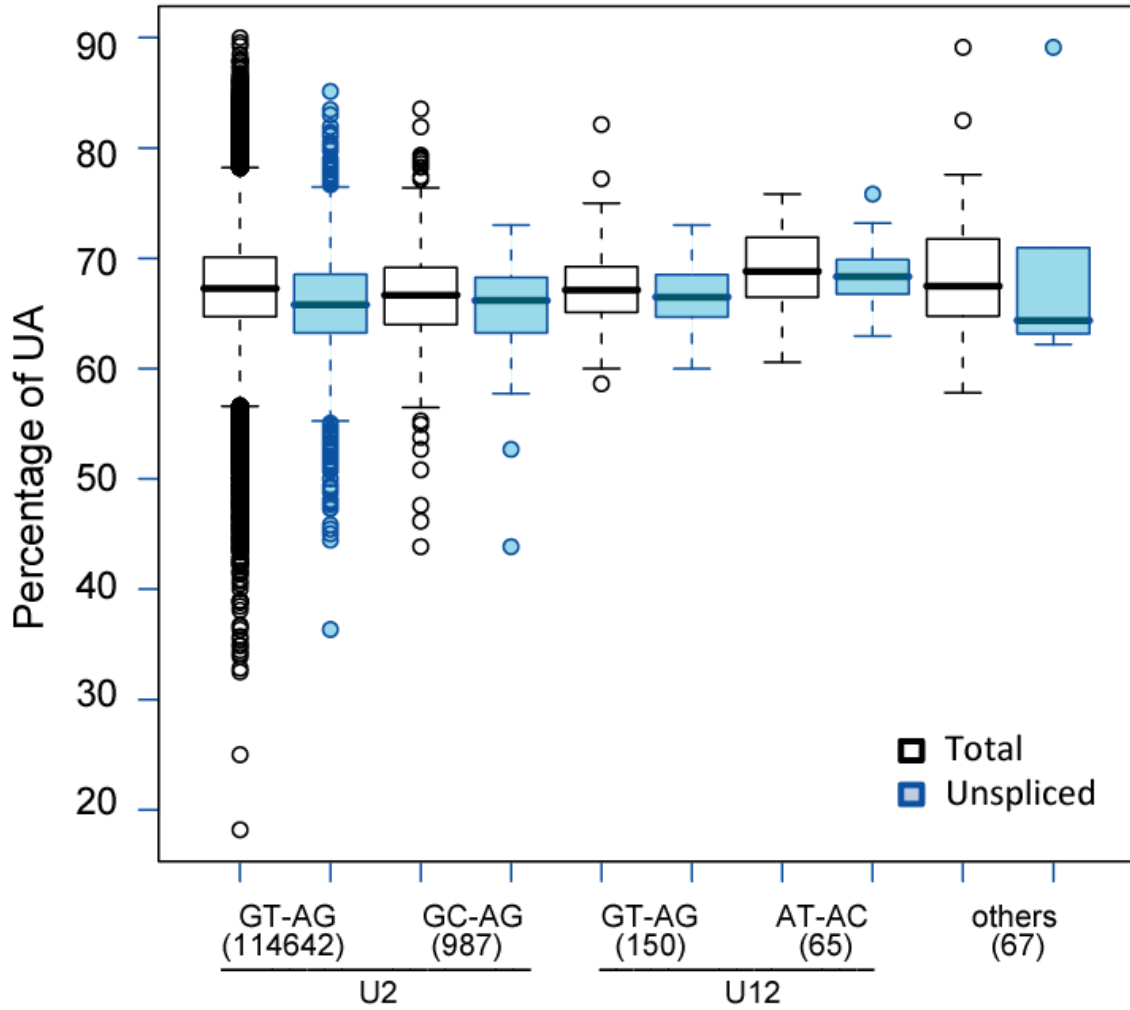


**Figure S10.** Slightly reduced UA richness in retained introns.

Box plot shows percentage of U and A bases for all introns of expressed genes and for retained introns. Both groups are divided into intron subtypes.

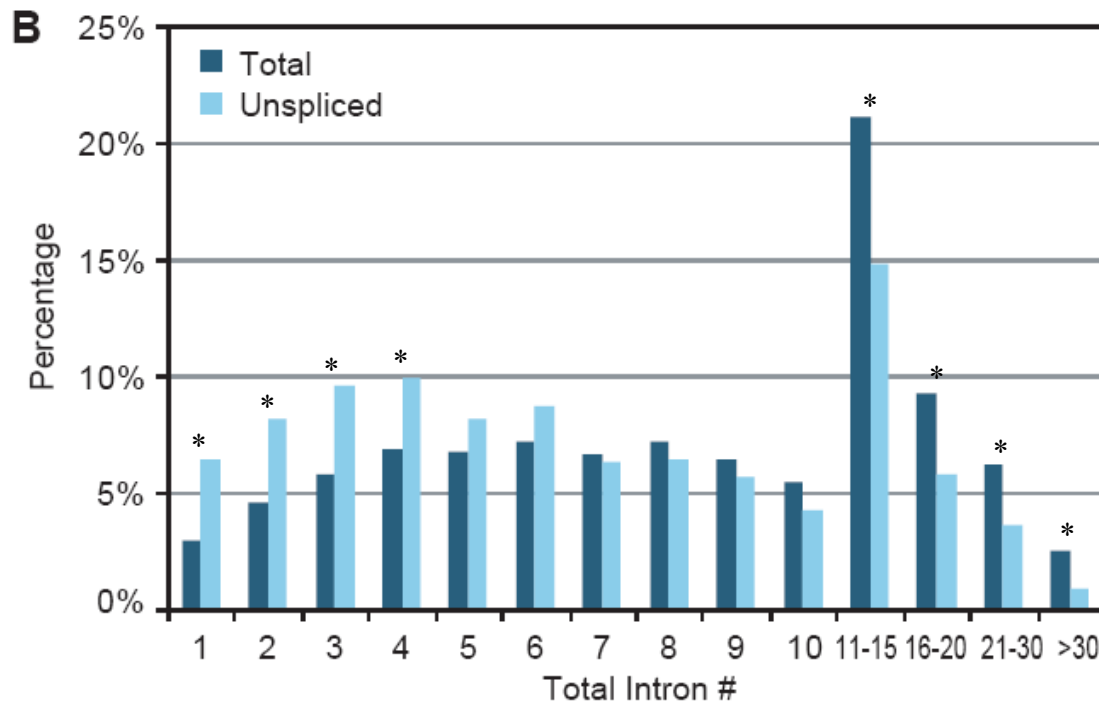
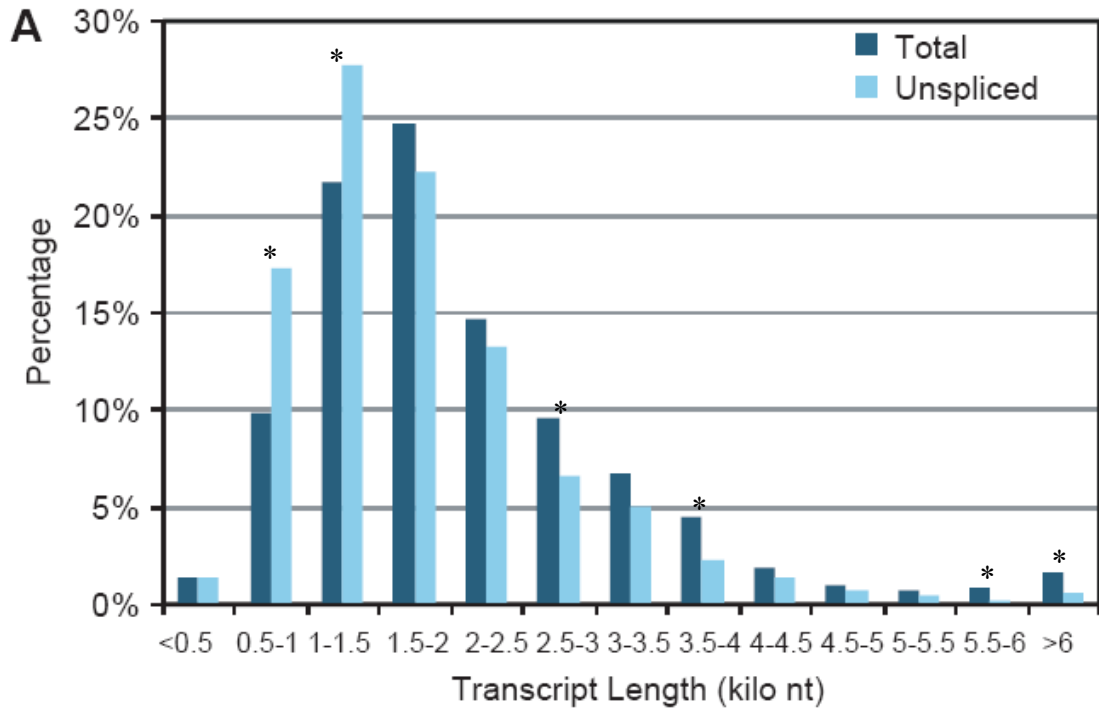


**Figure S11.** Correlation of gene transcript features and IR.

(A) Transcript length distributions of all expressed genes (dark blue) and of genes with retained introns (light blue) are shown. (B) Intron number distributions of all expressed genes (dark blue) and of genes with retained introns (light blue) are shown. Categories with FDR corrected chi-square test  $P < 0.001$  are marked with stars.



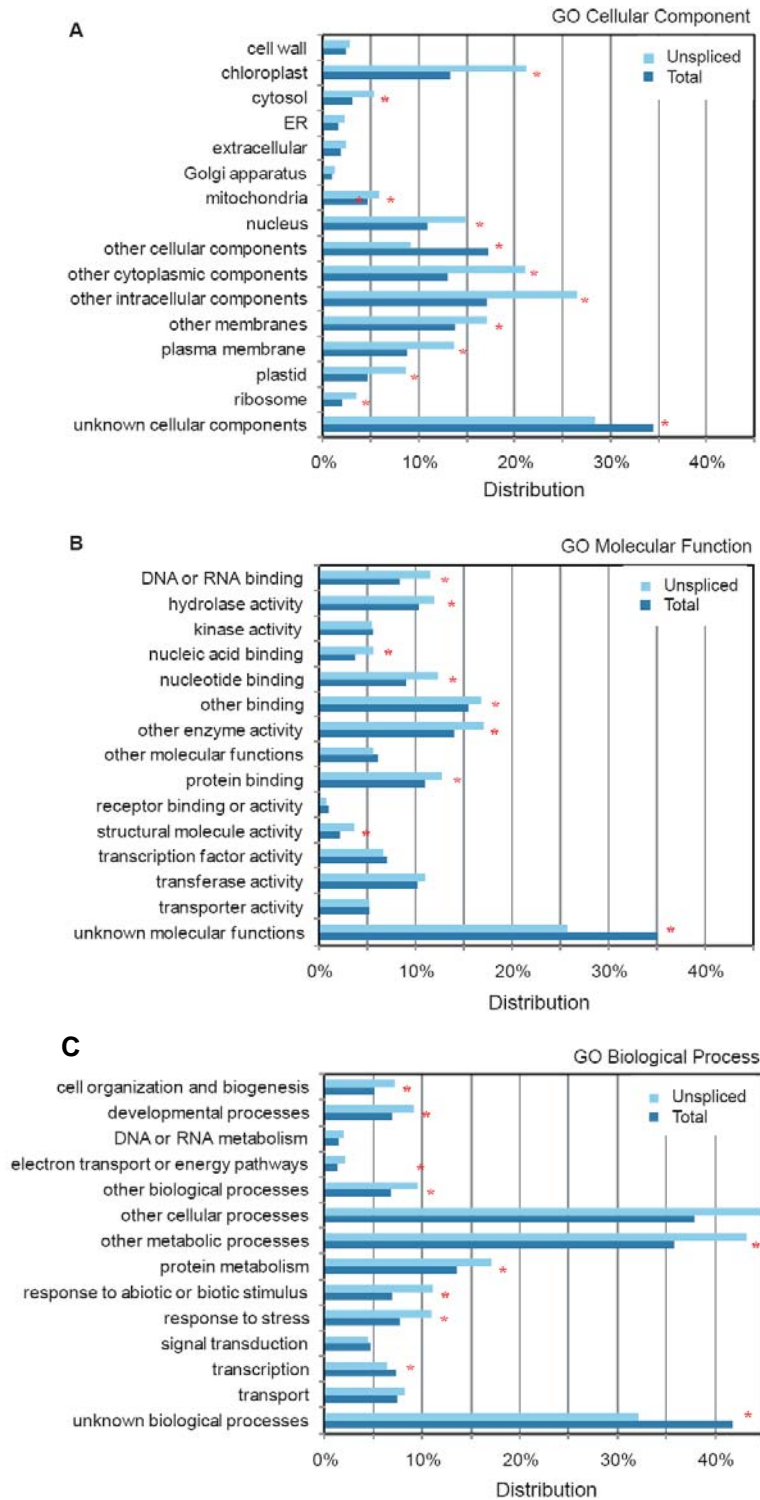


**Figure S12.** Relationship between gene function and IR.

Panels show functional classifications from GO annotation organized by Cellular Component (A), Molecular Function (B), and Biological Process (C). In each panel, all genes detected as expressed in the total mRNA population (dark blue) are compared with genes with retained introns detected (light blue). "Distribution" refers to the percentages of genes annotated to descriptive terms in a particular GO category divided by all genes. Categories with FDR corrected hypergeometric test  $P < 0.001$  are marked with stars.

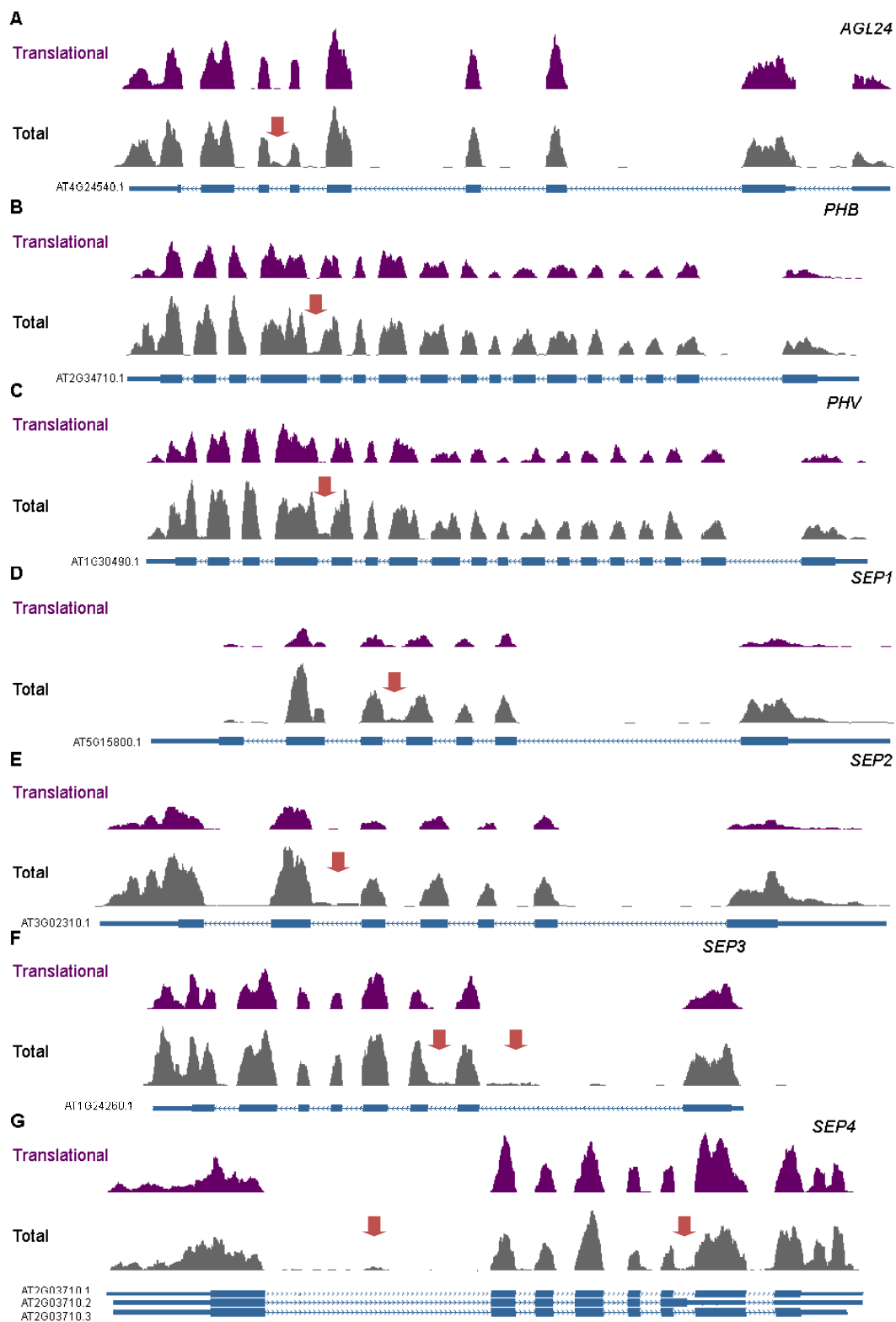


**Figure S13.** Fine-tuning of development-related genes.

Detection and quantification of retained introns in genes *AGL24* (A), *PHB* (B), *PHV* (C), *SEP1* (D), *SEP2* (E), *SEP3* (F), and *SEP4* (G) in stage 4 flower tissues. Total and translational RNAs were compared for each panel.

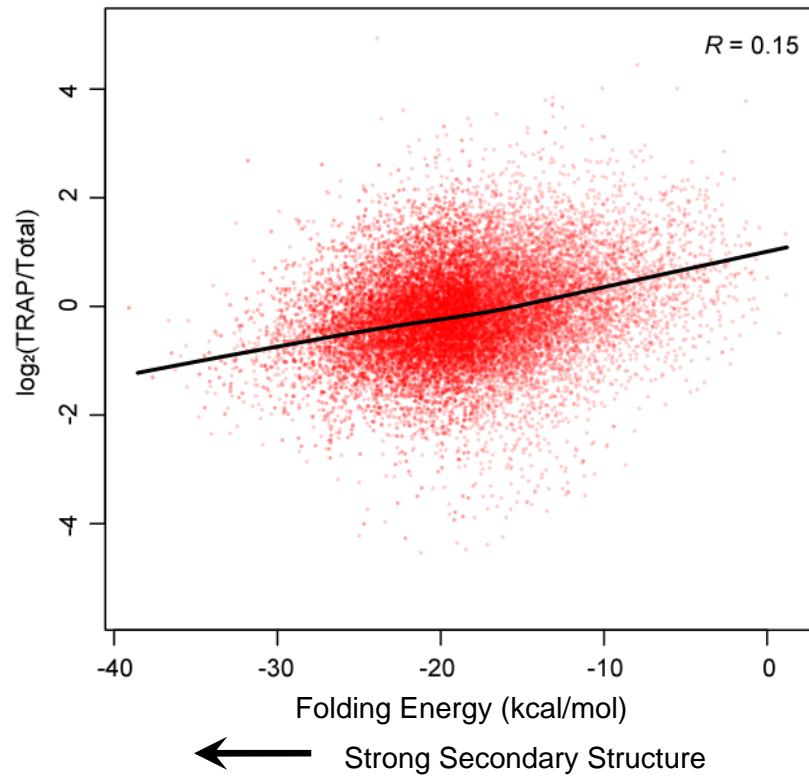
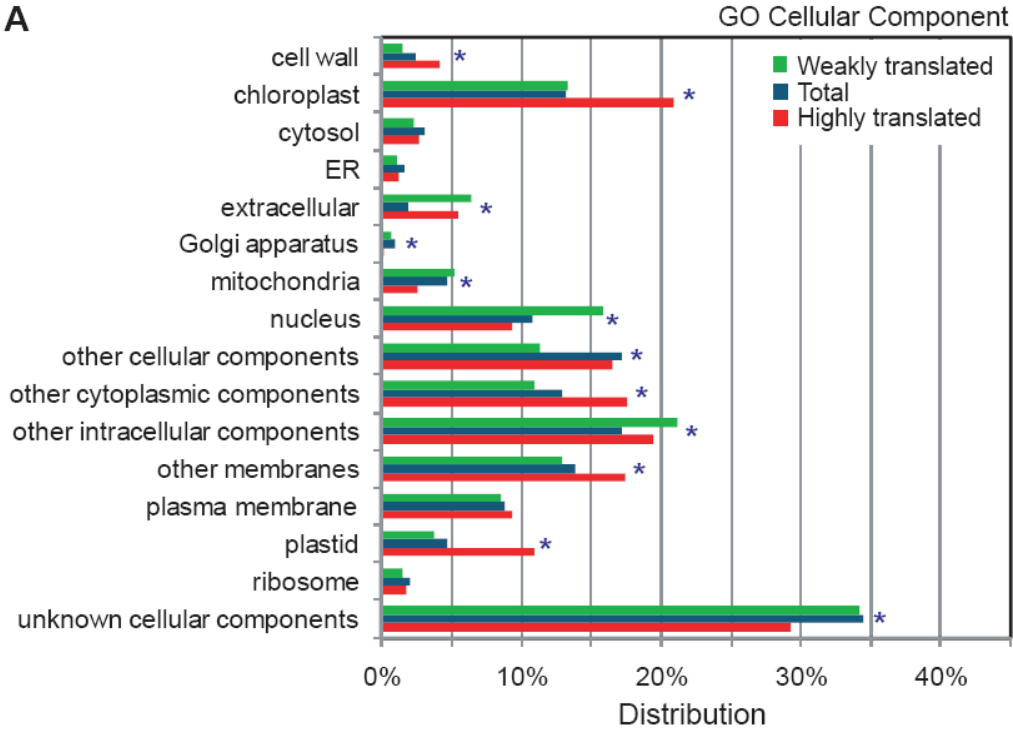


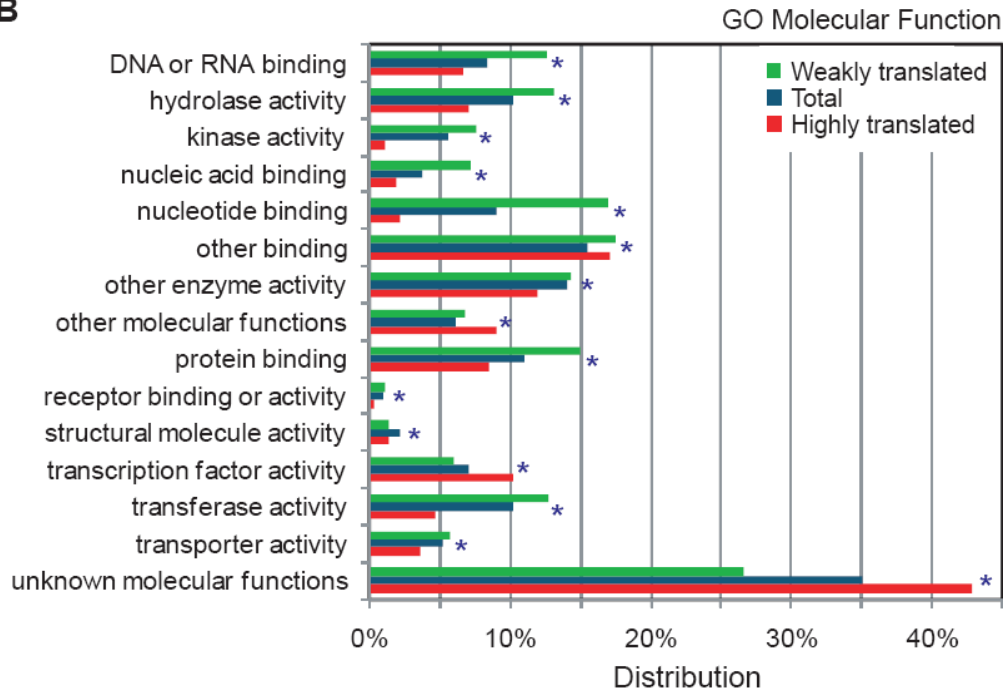
**Figure S14.** 5' mRNA folding energy correlates with translation state.

Predicted 5' mRNA folding energy was significantly correlated with translation state ( $R = 0.15$ ,  $P < 1E-4$ ). Folding energy was calculated for the first 60 nucleotides starting from the start codons.

**A**



**B**



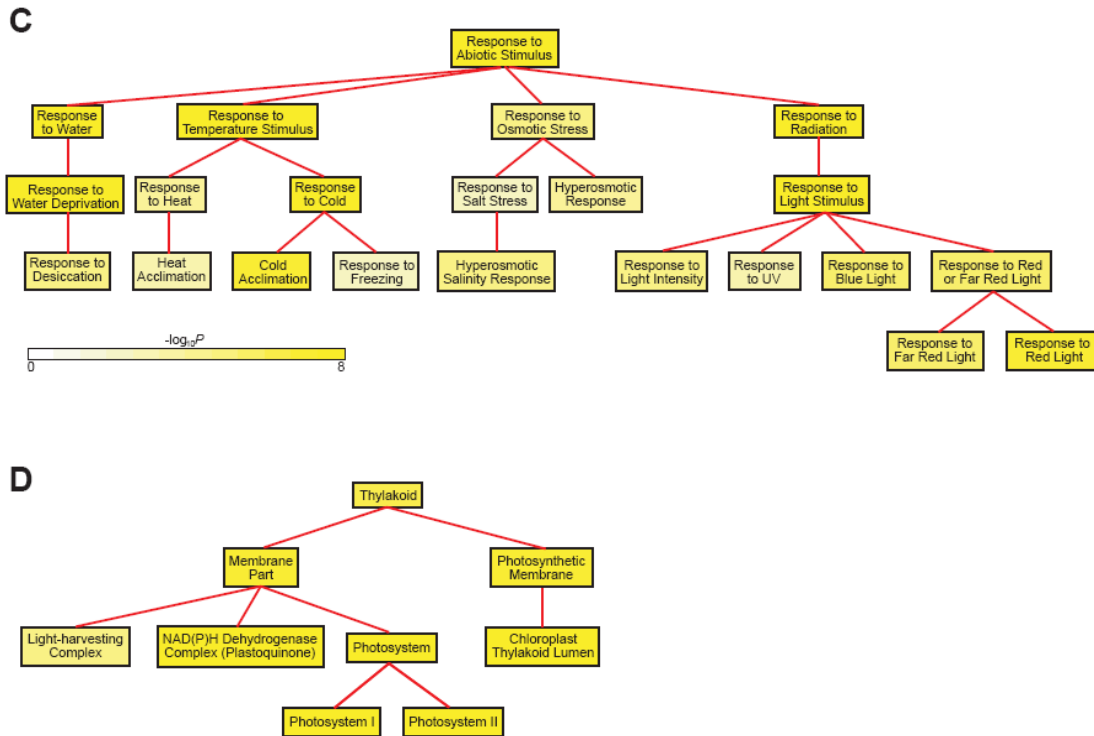


**Figure S15.** Relationship between gene function and translation state.

Panels show functional classifications from GO annotation organized by Cellular Component (A) and Molecular Function (B). In each panel, all genes detected as expressed in the total mRNA population (blue) are compared with highly ribosome bound genes (red) and weakly translated genes (green). "Distribution" refers to the percentages of genes annotated to descriptive terms in a particular GO category divided by all genes. Categories with FDR corrected hypergeometric test  $P < 0.001$  are marked with stars. Detailed GO analysis identifies significantly overrepresented ( $P < 0.001$ ) gene categories under "Response to Abiotic Stimulus" (C) and genes whose products locate in "Thylakoid" (D) for highly translated genes in floral organs at flower 4. Color bar: significance level for categories by hypergeometric test with FDR correction.

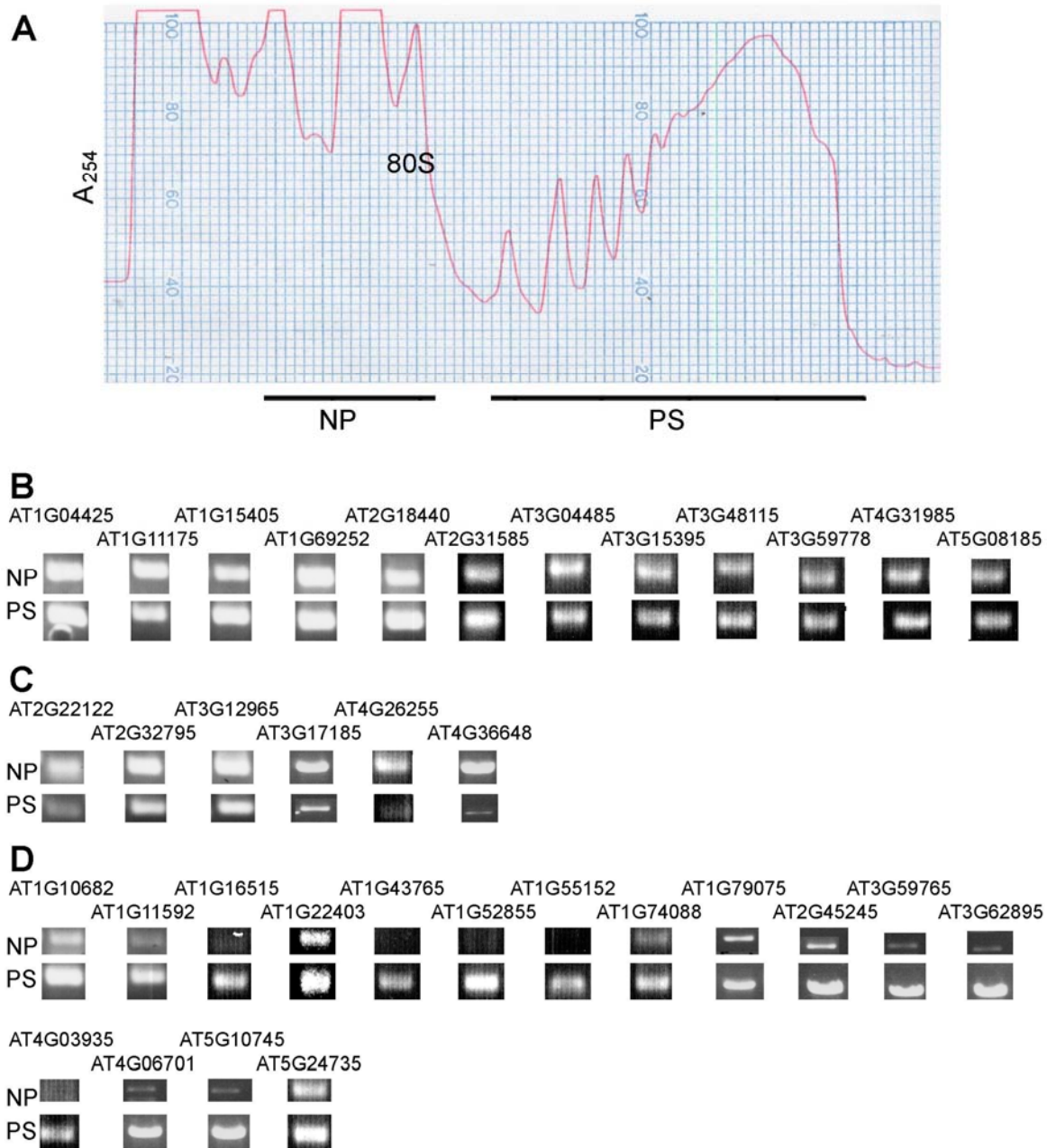


**Figure S16.** Semi-quantitative RT-PCR analysis of ribosome-associated ncRNA.

(A) Representative 254 nm UV absorbance profile for flower stage 6-7 ribosomes without *HF-RPL18* transgenline fractionated by ultracentrifugation through 20% to 60% (w/v) sucrose density gradients. NP RNA complexes fractionated in the top half of the gradient and PS RNA complexes fractionated in the bottom half of the gradient. (B-D) Total RNA isolated from NP and PS fractions were subjected to RT-PCR amplification with gene-specific primers for ncRNA. The PCR products were separated in a 2% (w/v) agarose gel. Tested ncRNA have similar abundance in the NP and PS fractions (B), enriched in the NP fraction (C), or enriched in the PS fraction (D).